Indentation as a probe for pressure sensitivity of metallic glasses

2008 J. Phys.: Condens. Matter 20 114119

(http://iopscience.iop.org/0953-8984/20/11/114119)

IOP PUBLISHING JOURNAL OF PHYSICS: CONDENSED MATTER

J. Phys.: Condens. Matter **20** (2008) 114119 (7pp) doi:10.1088/0953-8984/20/11/114119

Indentation as a probe for pressure sensitivity of metallic glasses

Vincent Keryvin

LARMAUR, FRE-CNRS 2717, Université de Rennes 1, Campus de Beaulieu, 35042 Rennes, France

E-mail: vincent.keryvin@univ-rennes1.fr

Received 30 August 2007, in final form 15 October 2007
Published 20 February 2008
Online at stacks.iop.org/JPhysCM/20/114119

Abstract

The question of hydrostatic pressure or normal stress dependence of the flow and fracture behaviour of bulk metallic glasses is addressed. Data from several types of mechanical tests indicate that flow is hardly sensitive to pressures or normal stresses, while fracture is normal stress sensitive and not pressure dependent. Besides, instrumented indentation adequately probes a low pressure dependence of flow, while a normal stress dependence is hardly noticeable.

(Some figures in this article are in colour only in the electronic version)

1. Introduction

Metallic glasses, or amorphous alloys, have been produced in bulk form since the early 1990s [1, 2] allowing us to perform the usual mechanical tests. Some attention has been devoted to the influence of hydrostatic pressures or normal stresses on the behaviour of these alloys (see for instance [3–9]). Indeed, unlike conventional crystalline metallic alloys, whose plastic flow is only sensitive to shear, bulk metallic glasses (BMGs) may be sensitive to non-deviatoric terms of the stress tensor. The present paper's aim is first to briefly review the experimental mechanical results that address the question of the influence of pressure or normal stress on the flow and fracture properties of these alloys. Then, in a second part, the ability of the indentation test to adequately probe any kind of pressure sensitivity will be investigated vis-à-vis the conclusions of the first part.

2. Review of pressure effects on the flow and fracture properties of metallic glasses

2.1. Physical origins of pressure sensitivity

The origins of the pressure dependence of flow and fracture in metallic glasses are to be looked for at the atomistic scale. Metallic glasses have mainly metallic bondings so that strain can be accommodated through changes in neighbourhood more easily than in covalent or ionic solids [10]. Unlike other crystalline metals or alloys, they do not exhibit long-range translational symmetry. Plastic deformation in crystalline metals or alloys is linked to the crystal dislocations motion. In metallic glasses, plastic deformation is a not fully resolved topic. A local microscopic rearrangement of atoms must occur to accommodate shear and mainly two theories depict this scheme. The free-volume model applied to glass deformation [11] is a diffusion-like concept where atoms jump to vacant positions (free volume). The shear-transformation zone model [12] considers a local cluster of atoms that undergo an inelastic strain and goes from a low energy configuration to another one, crossing transiently an activated configuration of higher energy and volume. Both concepts are dilatational not only during the transient state between two low energy configurations but also in a permanent way, so that some pressure sensitivity is at stake. Another key point is that metallic glasses show very high macroscopic elastic strains (around 2%) so that local dilatational effects become important, in contrast to crystalline metals, where dislocations glide for around 0.1% strains on closely packed planes.

2.2. Yield and fracture criteria

A yield criterion describes when the material is no longer in the pure elastic state and enters a plastic (or inelastic state). For crystalline metallic alloys, flow onset is activated only by shear: there is no influence of pressure of any kind. In solid mechanics, pressure dependence can be described either as a mean stress dependence or a normal stress dependence.

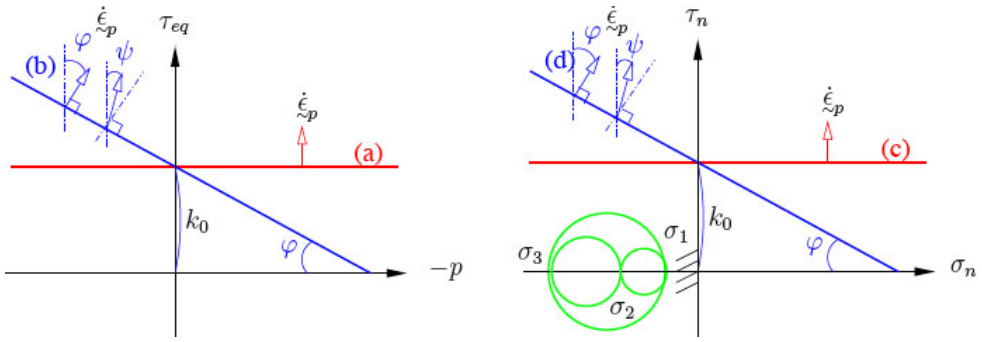

Figure 1. Yield criteria in the τ–σ plane (left), (a) von Mises's criterion and (b) Drucker–Prager's criterion, or in the Mohr's plane (right, σ_1, σ_2, σ_3 are the principal stress values), (c) Tresca's criterion and (d) Mohr–Coulomb's criterion.

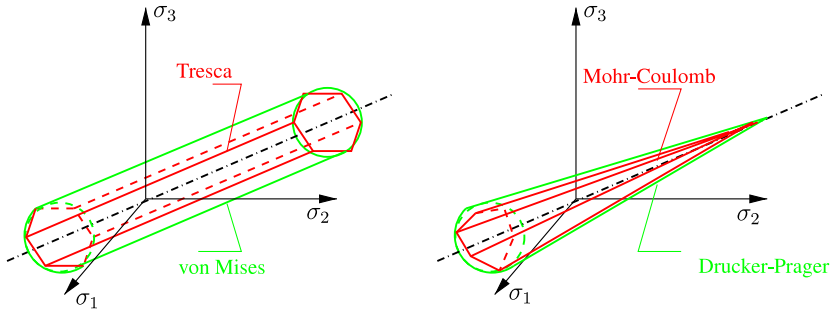

Figure 2. Yield criteria in the Haigh–Westergaard space (principal stresses space).

The stress tensor $\underset{\sim}{\sigma}$ can be divided into a deviatoric part, the shear stress tensor $\underset{\sim}{\tau}$, and a hydrostatic part σ_m (the opposite of pressure p) as

$$\underset{\sim}{\sigma} = \sigma_m \underset{\sim}{I} + \underset{\sim}{\tau} = -p \underset{\sim}{I} + \underset{\sim}{\tau}; \qquad \sigma_m = \tfrac{1}{3} \operatorname{tr} \underset{\sim}{\sigma}, \tag{1}$$

where $\underset{\sim}{I}$ is the second-order unit tensor and $\operatorname{tr} \underset{\sim}{\tau} = 0$ (tr is the trace operator). A yield criterion, that depends only on the two first invariants of the stress tensor and not on the third one, can be studied in a plane called the shear-pressure plane (see figure 1). The equivalent shear stress τ_{eq} is a mean of all shear stress components:

$$\tau_{\text{eq}} = \sqrt{J_2^\tau}; \qquad J_2^\tau = \tfrac{1}{2} \operatorname{tr}(\underset{\sim}{\tau} \cdot \underset{\sim}{\tau}). \tag{2}$$

Pressure-independent materials in terms of flow onset have therefore an elastic domain bounded by a horizontal line. This yield criterion is known as the Huber–von Mises' criterion (VM), where flow occurs only because of shear at a yield value of k_0:

$$\tau_{\text{eq}} = k_0. \tag{3}$$

A material with a pressure-sensitive yield criterion will then not be represented by a horizontal line. For example, if a linear dependence is assumed, we get the Drucker–Prager's criterion (DP), also used in geomechanics and for porous media. In this, flow onset will be eased by a positive mean stress and made difficult by pressure:

$$\tau_{\text{eq}} = k_0 + \tan\varphi \cdot p = k_0 + \beta \cdot p, \tag{4}$$

where k_0 and φ are respectively called the cohesive stress and the friction angle. Another way to describe flow onset is given by the concept of normal σ_n and tangential τ_n stresses. If flow occurs along a particular slip plane, of normal $\vec{n}$, along a given direction $\vec{t}$, one can define

$$\sigma_n = \vec{n} \cdot \underset{\sim}{\sigma} \cdot \vec{n}; \qquad \tau_n = (\underset{\sim}{\sigma} \cdot \vec{n} - \sigma_n \vec{n}) \cdot \vec{t}. \tag{5}$$

A yield criterion can be represented in the Mohr's plane τ_n–σ_n (see figure 1). For crystalline metallic alloys, there is no influence of the normal stress on flow onset. As a consequence the yield criterion is a horizontal line called Tresca's criterion. The necessary shear for flow is k_0 (the maximum resolved shear stress) whatever the normal stress.

$$\tau_n = k_0. \tag{6}$$

In contrast, if there is a dependence of flow on both normal and shear stresses, the yield criterion is no longer a horizontal line. For example, if there is a linear dependence on the normal stress, we have the Mohr–Coulomb's criterion (MC). This time the necessary shear for flow is the maximum shear stress decreased by a positive normal stress (in tension for example) and increased by a negative one (for example in compression).

$$\tau_n = k_0 + \tan\varphi \cdot \sigma_n = k_0 - \alpha \cdot \sigma_n, \tag{7}$$

where k_0 and φ are respectively called the cohesive stress and the friction angle (they are *a priori* slightly different from the DP ones). Both DP and MC criteria incorporate a dependence on hydrostatic components of the stress tensor, and the differences are of the same kind as those between Tresca and von Mises criteria. This is illustrated by figure 2,

Table 1. Strengths of two metallic glasses (Vit1 stands for $Zr_{41.25}Ti_{13.75}Cu_{12.5}Ni_{10}Be_{22.5}$ at.%) in tension (Y_t), compression (Y_c), plane-strain compression (Y_{psc}), pure shear (k) and fracture angles in tension (θ_t) and compression (θ_c).

Alloy	Y_t (GPa)	Y_c (GPa)	Y_{psc} (GPa)	k (GPa)	θ_t (deg)	θ_c (deg)
Vit1 [4]	1.89	1.93	2.12	1.03	55	$\simeq$45
$Pd_{40}Ni_{40}P_{20}$ (at.%) [3]	1.45	1.78	1.75	0.795	50	41
$Pd_{40}Ni_{40}P_{20}$ (at.%) [13, 14]	1.6	1.7	—	—	56	42

where the four yield criteria are drawn in the principal stresses space. Tresca and von Mises criteria are both represented by cylinders along the hydrostatic pressure axis: the VM criterion is generated by a circle and Tresca's criterion by a regular hexagon. The same situation holds for MC and DP criteria, which are both represented by cones along the hydrostatic pressure axis: DP is generated by a circle and MC by an irregular hexagon. MC and Tresca criteria incorporate a dependence on the third invariant of the deviatoric stress (dependence on the angle in the deviatoric plane), which DP or VM criteria do not. Although DP and MC criteria both exhibit a possible asymmetry in compressive and tensile yield strengths (which VM and Tresca criteria would not), they differ on some points. First, for MC the slip plane may deviate from the plane of maximum resolved shear stress (45° vis-à-vis the loading axis in tension or compression), while for DP the orientation of the slip plane is not altered. Second, in a plane strain compression test for example (carried out by increasing the contact friction between the specimen end and the platen and by lowering the aspect ratio of the sample), MC will give the same strengths as in pure compression while for DP the results may differ.

Fracture criteria can be represented by surfaces like yield criteria. The main difference is that instead of predicting the onset of flow they predict the onset of fracture. Often yield and fracture criteria are confused. This is due to the fact that in uniaxial tension or compression bulk metallic glasses are brittle or quasi-brittle (without strain-hardening) so that yield strengths equal fracture strengths. One feature that is able to differentiate yield and fracture criteria concerns the angles formed by fracture surfaces or shear bands vis-à-vis a loading direction. The former case will give some hints on the fracture criterion, while the latter one will deal with a yield criterion.

2.3. Experimental evidence for pressure sensitivity

In table 1 are summarized the results of uniaxial tests conducted on a Zr-based and a Pd-based BMG [4, 3, 13, 14] including torsion, tension, compression and plane-strain compression. For the Vit1 alloy, there is no real asymmetry of yield strengths in tension and compression and a VM yield criterion can capture all these data. The authors [4] therefore concluded on an absence of pressure or normal stress dependence for yielding. For the Pd-based glass, Donovan [3] concluded that a MC yield criterion with a normal stress dependence was relevant while a pressure-dependent yield criterion was not, because of the same strength values obtained in compression, plane strain compression and pure shear (obtained by antisymmetric four point bending). She obtained (see equation (7)) $\alpha = 0.113$ by comparing shear and compression results (0.096 between shear and plane strain compression). Therefore, a contrary conclusion to the Vit1 data was made! As a general remark, all these mechanical tests are not so easy to perform for brittle materials with such high strengths as BMG. Tension tests are highly sensitive to surface defects or bulk defects (such as oxides in Zr-based alloys [15]). Compression tests are highly sensitive to both friction at the ends and misalignment of the load, possibly giving too low results. Plane-strain compression tests are not homogeneous, so interpretation of results can be difficult. Moreover, even the slight asymmetry in tensile and compressive strengths may be compromised by the fact that, as BMGs exhibit very high yield strains (around 2%), nominal stress values must be corrected to give true stress values, decreasing the compressive yield strength and increasing the tensile one, thus reducing this slight asymmetry. In addition, for the Pd-based glass, some testing methods can be imprecise: as an example, Donovan used bending tests to get the tensile yield strength. Mukai *et al* [13, 14], on the same alloy, obtained higher tensile yield strengths, still making the MC criterion qualitatively relevant but not quantitatively consistent with all data. In this case a negative value of α is obtained! Therefore, it is difficult to conclude from these data for the Pd-based glass whether a normal stress yield criterion or a pressure-dependent one is relevant.

Data on fracture angles may provide hints for making a correlation between the same experiments and a fracture criterion. As already stated, only MC can predict a deviation from 45°. For both glasses we have a subsequent deviation from 45° in tension and a slight or no deviation in compression. This means that a normal stress-dependent fracture criterion such as MC is relevant. However, the asymmetry of the fracture angles in tension and compression cannot lead to a single slope MC fracture criterion [16]. Nevertheless, as stated by Rudnicki and Rice [17], and recalled recently by Anand and Su [18], the fracture angle depends not only on the friction angle φ but also on the dilatancy angle ψ (see figure 1). It is therefore possible to use a non-associative flow rule (the direction of the plastic strain rate tensor $\dot{\underset{\sim}{\epsilon}}_p$) with dilatancy ψ as a function of the stress state, in our case the normal stress, to take into account the asymmetry between the fracture angles in tension and compression. Recently, Anand and Su [18] proposed such a model and found consistent values for these angles on the Vit1 glass between tension and compression data and finite element analyses. However, recently, Sunny *et al* [19] considered a novel design for compressive samples subjected to high strain rates to prevent failure to initiate at the sample ends and to make it start in the gauge length. They found that the fracture angle

in compression (50°) for the Vit1 alloy was very similar to previous studies of Lewandowski and Lowhaphandu [5] in tension (50°–59°). Therefore, a simple MC fracture criterion (with only one slope) may be relevant whatever the sign of the normal stress.

Data from multiaxial stress state experiments on the Vit1 alloy are also available in the literature. Lewandowski and Lowhaphandu [5] performed some tension and compression tests with additional pressures up to 700 MPa. Their results suggested a very low dependence of yield strengths on pressure. These results have been recently extended to pressures up to 1.5 GPa with the same conclusions [20]. The fracture angles deviate both in tension and compression but again their values were not significantly changed by pressure. Nearly at the same time, Lu and Ravichandran [21] performed some multiaxial compression experiments, on the same alloy, with a confining sleeve apparatus giving hydrostatic pressures up to 2.8 GPa. They found, this time, a pronounced influence of high pressure on yield strengths. However, their results may be compromised by friction, which may explain this discrepancy with Lewandowski and co-workers [5, 20]. It was also found that shear bands on the outer edges of their unbroken specimens were oriented at 45° from the compressive load so that the normal stress had no influence on shear bands angle.

On the same Vit1 alloy, Flores and Dauskardt [22] performed some toughness tests in opening mode, called mode I, and in shear mode, called mode II. They found toughness values around 20 MPa $m^{1/2}$ in mode I and nearly four times higher in mode II. It is known that in the case of brittle materials the mode II fracture toughness is greater than the mode I toughness, because the micromechanism of fracture is stress controlled, with the normal crack tip stress controlling the fracture process. In contrast, ductile metals have lower mode II toughness values, because the crack tip fracture process is shear strain controlled (dislocation glide). Increased shear lowers the resistance to fracture under mode II loading. The results on the Vit1 glass thus indicate a major influence of normal stress in fracture.

A last search for pressure sensitivity, even if not experimental but able to be linked to its atomistic origin, was made by Lund and Schuh [23] with some molecular dynamics simulations on a model binary metallic glass. They found that a Mohr–Coulomb criterion can capture some runs with biaxial stress states while a Tresca criterion cannot.

As a summary of some of the available experimental data on flow and fracture of metallic glasses, two main points need to be considered. First, it is not clear that the tension/compression asymmetry of yield strengths should be regarded as a general rule for BMGs. Moreover, an isotropic yield criterion like VM, therefore pressure insensitive, can be very close to experimental data coming from different types of loadings, even for high pressures. Second, fracture angles deviating from the maximum resolved shear angle bring a natural conclusion on a normal stress fracture criterion like MC, not sensitive to even high pressures.

The second part of this paper will analyse indentation results in regard to these conclusions.

Table 2. Mechanical and physical properties of the $Zr_{55}Cu_{30}Al_{10}Ni_5$ BMG: d is density measured by Archimedes' technique, E (Young's modulus) and ν (Poisson's ratio) are determined by ultrasonic echography, Y_t and Y_c are the yield stresses in tension and in compression respectively [25] and T_g is the glass transition temperature determined by thermal expansion measurements at 5 K min^{-1} [26].

d	E (GPa)	ν	Y_t (GPa)	Y_c (GPa)	T_g (K)
6.83	84.4	0.364	1.6	1.8	673

3. Indentation as a probe for pressure sensitivity

3.1. Indentation background

Instrumented sharp indentation consists in applying a load to a flat and polished surface via a conical or pyramidal indenter. Both the applied load P and the displacement h under the indenter are continuously monitored, giving the test mechanical response as the P–h curve. After unloading, the mean contact pressure or Meyer's hardness H is computed as the ratio between the maximum applied load and the projected area of contact measured with the geometrical characteristics of the residual print. Two deformation regimes may exist under a sharp indenter [24]. In the elasto-plastic regime, the plastic zone develops under the indenter but does not completely surround it: hardness, in this case, is not a material property and depends on the indenter geometry (for example for low apex angle cones). In the fully plastic regime (for high apex angle cones), the plastic zone completely surrounds the indenter: it is a self-similar regime where hardness and the constraint factor C (the ratio of H to the compressive yield strength Y_c, this latter being taken as constant for non-hardening materials like BMGs) are, this time, material parameters. Apart from the very small volumes of material necessary to perform the test, the indentation test is a constrained deformation test, that offers the possibility to study the development of flow, which is precluded in uniaxial tests like tension or compression where the behaviour is brittle. Moreover, both very high pressures and a high multiaxial stress state exist below the indenter and this gives the opportunity to study the pressure dependence and to compare with multiaxial tests.

3.2. Experimental and numerical procedures

Indentation tests were performed on a $Zr_{55}Cu_{30}Al_{10}Ni_5$ (at.%) bulk metallic glass whose mechanical and physical properties are reported in table 2. Diamond conical (apex angles from 90° to 148°) and pyramidal (Vickers, Berkovich, see [27] for a description) indenters are used. Specimens are mirror-polished by standard metallographic techniques using SiC and diamond containing grids. Hardness H was systematically computed by measuring the print dimensions by confocal microscopy. Plastic deformation mechanisms under the indenter are investigated by the bonded interface technique [28–30], that is more adequate for BMGs than direct observation (non-transparency) or breaking after indentation along radial cracks (this BMG does not crack during indentation). Specimens were

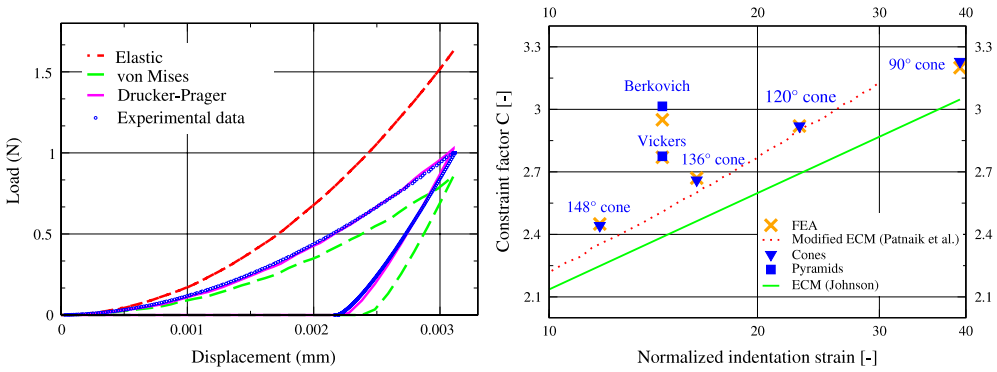

Figure 3. (a) Load–displacement curves of a 1 N Vickers indentation experiment. Comparisons between experimental data and FE simulations using different behaviour laws. (b) Constraint factor versus normalized indentation strain (x-axis is logarithmic scale): experimental data, numerical simulations (FEA) for the conical and pyramidal indenters compared to elasto-plastic regime expanding cavity models (ECMs).

prepared by bonding two pieces together, already polished to a 1 μm finish, then were clamped in a special device to reduce the bond thickness. Following this, the top surface of the bonded specimen was polished carefully so that the indentation face is flat. Vickers diamond indentations were performed both on the bonded interface as well as away from it in the bulk for comparison. Indentations on the interface were conducted in such way that the indentation diagonals (for the Vickers pyramid) coincides with the interface, whose thickness was in best cases 2 μm thick. Finite element simulations of the indentation response of bulk metallic glasses are undertaken (see details in [25]). An associative elasto-perfectly-plastic Drucker–Prager behaviour law is used for the BMG (see figure 1). For all simulations, hardness is computed by measuring the surface profiles at full applied load.

3.3. Results and discussion

A comparison of the load–displacement curve between experimental and simulated data is presented in figure 3(a). It can be observed, as already reported [7, 8, 25], that an influence of hydrostatic (or normal [7]) stress terms must be taken into account to match the data.

The constraint factor is reported for the different indenters versus a normalized indentation strain (a representative strain depending on the indenter geometry over the yield strain) proposed by Johnson [24] in figure 3(b). The two indentation regimes are clearly visible. The elasto-plastic regime shows an increasing constraint factor (for cones over 120° apex angle and the pyramids) while, for the fully plastic regime, one has a constant value around 3.2. (Note that the x-position of the pyramid data is wrong because a classical equivalent conical angle of 140.6° was taken; data should be shifted to the right [25].) It is known that elasto-perfectly plastic materials with no pressure dependence have constraint factors around 2.7–2.8 [31]. Constraint factors above 2.8 for pressure-dependent materials such as soils have been reported; therefore, the BMG shows a pressure sensitivity by its high constraint factors. For the elasto-plastic regime of indentation, Johnson [24] proposed a model based on the results of a hollow sphere under internal pressure (expanding cavity model, ECM). This model is a straight line in a semi-logarithmic plot. Experimental data for the BMG lie slightly above this curve. Recently, Narasimhan [32, 8] revisited the ECM with the Drucker–Prager behaviour law and has seen an increase in C with the pressure dependence of the yield criterion. His model, for a friction angle of 10° (directly computed from the tensile and compressive strengths), agrees very well with our experimental data in the elasto-plastic regime. FE simulations have also been made for some selected conical and pyramidal tests. A remarkable agreement is found between the experimental data and these simulations.

It is also possible to link the plastic zone size with pressure sensitivity. This plastic zone is the zone where there are shear bands around and underneath the print as evidenced in figure 4. This is what Ramamurty and co-workers did on a Pd-based glass and the Vit1 alloy under a Vickers indentation [29, 30, 33, 34]. They observe that the plastic zone is hemispherical as evidenced in figure 4(a). This can give credit to the expanding cavity model idea used by Johnson [24]. However, the plastic zone size given by Johnson greatly overestimates the experimental data, suggesting an increase of the yield strength because of the very high pressures (around twice the initial yield strength). Ramamurty *et al* [33], by taking the results of multiaxial tests of Lu and Ravichandran [6] on the Vit1 alloy, showed that such an increase could quantitatively match the experimental plastic zone size.

Underneath the print, two types of shear bands are seen (see figure 4(a)): semi-circular ones resulting from out-of-plane shear (artefacts due to the bonding technique) and some radial ones (in-plane shear) that should represent what really takes place during indentation in the bulk. These latter bands do intersect at a given angle (here around 90° as seen in figure 4(a)). In the axisymmetric cases, prints show, at the surface, two types of shear bands (see figure 4(b)): some circular ones and some in spiral-like shapes [25]. The latter bands also tend to intersect at a given angle (here around 94° as seen in figure 4(b)). Let us note that this angle is quite difficult to measure with accuracy and confidence. Using the theory of slip-line fields, if the material has no normal stress dependence, this angle should be 90°. This was found for

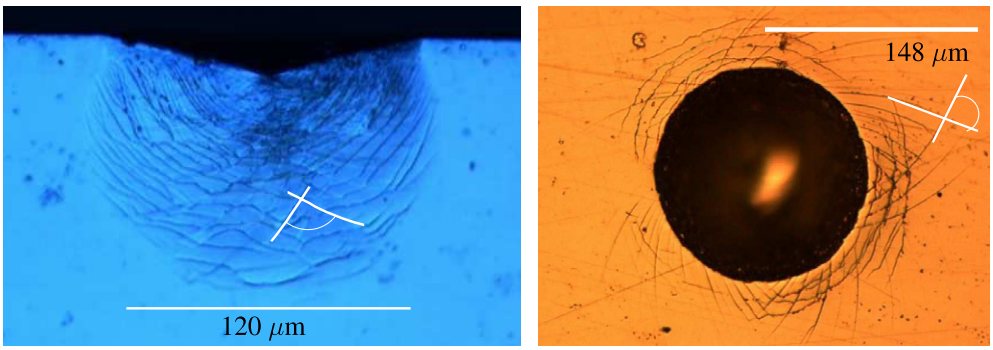

Figure 4. Optical micrographs of (a) the plastic zone underneath a 5 kg Vickers indentation by the bonded interface technique. (b) Shear bands around a 100 N 90° conical indentation.

spiral bands at the surface in a Zr-based alloy by Trichy *et al* [35]. In contrast, if the angle is different from 90°, the friction angle (in the MC criterion, see figure 1) can be extracted as for example on the Vit1 glass [8]. Anand and Su [18] recently studied the intersection of the shear bands during indentation, underneath the indenter, by a blunted wedge with a bonded interface technique and found 84° on a Zr-based alloy. In view of this variety of results, no evidence may be given that a direct correlation exist between this angle and the friction angle. However, Anand and Suh [36] found a remarkable correlation between their experimental angle value and some FE simulations with a normal stress-dependent model with account for dilatancy.

Therefore, it seems that indentation probes a pressure sensitivity of flow. The apparent discrepancy between multiaxial experiments, where the effects of pressure were hardly noticeable, and indentation tests may lie in the existence of higher pressures (that are at least higher than the mean contact pressure or hardness, 5.1 GPa for the Zr-based BMG studied here [25]) under the indenter tip than for multiaxial tests. The small slope of pressure dependence obtained for low pressures may lead to a higher pressure sensitivity for very high pressures.

4. Conclusions

The question of pressure (or normal stress) sensitivity of flow and fracture in metallic glasses has been addressed. Experimental mechanical tests and their interpretations have been briefly reviewed. They seem to indicate that flow is rather shear controlled, so that a yield criterion like the von Mises can be adequate, while fracture is normal stress controlled, so that a fracture criterion like the Mohr–Coulomb can be relevant. In both cases, no strong influence of hydrostatic pressures can be clearly evidenced. Some indentation experiments, where very high pressures are at stake, were performed on a Zr-based BMG. Results, as well as those of the literature, were challenged to the question of pressure sensitivity of flow. The mechanical response, as well as the relatively high constraint factor values, clearly shows a contribution to non-shear stresses to flow. Analyses of the shear-bands geometry and of the plastic zone shape raise some questions on a pressure or normal stress sensitivity even if these arguments need to be further investigated to give consistent conclusions. Nevertheless, instrumented indentation seems to be an appropriate tool for probing the pressure-dependent character of metallic glasses.

Acknowledgments

The author would like to thank Professor J-C Sanglebœuf, University of Rennes, France, for his experimental help, and Professor Y Yokoyama, Tohoku University, Japan, for providing the specimen.

References

[1] Inoue A, Zhang T and Masumoto T 1990 Zr–Al–Ni amorphous alloys with high glass transition temperature and significant supercooled liquid region *Mater. Trans.* **31** 177
[2] Peker A and Johnson W L 1993 A highly processable metallic glass: $Zr_{41.2}Ti_{13.8}Cu_{12.5}Ni_{10.0}Be_{22.5}$ *Appl. Phys. Lett.* **63** 2342
[3] Donovan P E 1989 A yield criterion for the $Pd_{40}Ni_{40}P_{20}$ metallic glass *Acta. Metall.* **37** 445–56
[4] Bruck H A, Christman T, Rosakis A J and Johnson W L 1994 Quasi-static constitutive behavior of $Zr_{41.2}Ti_{13.8}Cu_{12.5}Ni_{10.0}Be_{22.5}$ bulk amorphous alloys *Scr. Metall. Mater.* **30** 429–34
[5] Lewandowski J J and Lowhaphandu P 2002 Effect of hydrostatic pressure in the flow and fracture of a bulk amorphous metal *Phil. Mag.* **82** 3427–41
[6] Lu J, Ravichandran G and Johnson W L 2003 Deformation behavior of the $Zr_{41.2}Ti_{13.8}Cu_{12.5}Ni_{10.0}Be_{22.5}$ bulk metallic glass over a wide range of strain-rates and temperatures *Acta Mater.* **51** 3429–43
[7] Vaidyanathan R, Dao M, Ravichandran G and Suresh S 2001 Study of mechanical deformation in bulk metallic glass through instrumented indentation *Acta Mater.* **49** 3781
[8] Patnaik M N M, Narasimhan R and Ramamurty U 2004 Spherical indentation response of metallic glasses *Acta Mater.* **52** 3335
[9] Eswar Prasad K, Raghavan R and Ramamurty U 2007 Temperature dependence of pressure sensitivity in a metallic glass *Scr. Mater.* **57** 121–4
[10] Schuh C A, Hufnagel T C and Ramamurty U 2007 Mechanical behavior of amorphous alloys *Acta Mater.* **55** 4067–109

[11] Spaepen F 1977 A microscopic mechanism for steady state inhomogeneous flow in metallic glasses *Acta Metall.* **25** 407
[12] Argon A S 1979 Plastic deformation in metallic glass *Acta Metall.* **27** 47–58
[13] Mukai T, Nieh T G, Kawamura Y, Inoue A and Higashi K 2002 Effect of strain rate on compressive behavior of a $Pd_{40}Ni_{40}P_{20}$ bulk metallic glass *Intermetallics* **10** 1071
[14] Mukai T, Nieh T G, Kawamura Y, Inoue A and Higashi K 2002 Dynamic response of a $Pd_{40}Ni_{40}P_{20}$ bulk metallic glass in tension *Scr. Mater* **46** 43
[15] Keryvin V, Bernard C, Sanglebœuf J-C, Yokoyama Y and Rouxel T 2006 Toughness of $Zr_{55}Cu_{30}Al_{10}Ni_5$ bulk metallic glass for two oxygen levels *J. Non-Cryst. Solids* **352** 2863
[16] Zhang Z F, Eckert J and Schultz L 2003 Difference in compressive and tensile fracture mechanisms of $Zr_{59}Cu_{20}Al_{10}Ni_8Ti_3$ *Acta Mater.* **51** 1167
[17] Rudnicki J W and Rice J R 1975 Conditions for the localization of deformation in pressure-sensitive dilatant materials *J. Mech. Phys. Solids* **23** 371–94
[18] Anand L and Su C 2005 A theory for amorphous viscoplastic materials undergoing finite deformations, with application to metallic glasses *J. Mech. Phys. Solids* **63** 1362–96
[19] Sunny G P, Lewandowski J J and Prakash V 2007 Effects of annealing and specimen geometry on dynamic compression of a Zr-based bulk metallic glass *J. Mater. Res.* **22** 389–401
[20] Lewandowski J J 2007 private communication
[21] Lu J and Ravichandran G 2003 Pressure-dependent flow behaviour of $Zr_{41.2}Ti_{13.8}Cu_{12.5}Ni_{10.0}Be_{22.5}$ bulk metallic glass *J. Mater. Res.* **18** 2039–49
[22] Flores K M and Dauskardt R H 2006 Mode II fracture behavior of a Zr-based bulk metallic glass *J. Mech. Phys. Solids* **54** 2418–35
[23] Lund A C and Schuh C A 2003 Yield surface of a simulated metallic glass *Acta Mater.* **51** 5399–411
[24] Johnson K L 1985 *Contact Mechanics* (Cambridge: Cambridge University Press)
[25] Keryvin V 2007 Indentation of bulk metallic glasses: relationships between shear-bands observed around the prints and hardness *Acta Mater.* **55** 2565–78
[26] Keryvin V, Vaillant M-L, Rouxel T, Gloriant T and Kawamura Y 2002 Thermal stability and crystallisation of a $Zr_{55}Cu_{30}Al_{10}Ni_5$ bulk metallic glass studied by *in situ* ultrasonic echography *Intermetallics* **10** 1289
[27] Fischer-Cripps A C 2002 *Nanoindentation* (Berlin: Springer)
[28] Guiberteau F, Padture N P and Lawn B R 1994 Effect of grain size on hertzian contact damage in alumina *J. Am. Ceram. Soc.* **77** 1825
[29] Jana S, Ramamurty U, Chattopadhyay K and Kawamura Y 2004 Subsurface deformation during Vickers indentation of bulk metallic glasses *Mater. Sci. Eng.* A **375–377** 1191
[30] Jana S, Bhowmick R, Kawamura Y, Chattopadhyay K and Ramamurty U 2004 Deformation morphology underneath the Vickers indent in a Zr-based bulk metallic glass *Intermetallics* **12** 1097
[31] Cheng Y-T and Cheng C-M 2004 Scaling, dimensional analysis and indentation measurements *Mater. Sci. Eng.* R **44** 91
[32] Narasimhan R 2004 Analysis of indentation of pressure sensitive plastic solids using the expanding cavity model *Mech. Mater.* **36** 633
[33] Ramamurty U, Jana S, Kawamura Y and Chattopadhyay K 2005 Hardness and plastic deformation in a bulk metallic glass *Acta. Mater.* **53** 705
[34] Bhowmick R, Raghavan R, Chattopadhyay K and Ramamurty U 2006 Plastic flow softening in a bulk metallic glass *Acta. Mater.* **54** 4221
[35] Trichy G R, Scattergood R O, Koch C C and Murty K L 2005 Ball indentation tests for a Zr-based bulk metallic glass *Scr. Mater.* **53** 1461
[36] Su C and Anand L 2006 Plane strain indentation of a Zr-based metallic glass: experiments and numerical simulation *Acta Mater.* **54** 179